Climate Dynamics (2022) 59:2979–2994
https://doi.org/10.1007/s00382-022-06255-8

A tree ring-based hydroclimate reconstruction for eastern Europe reveals large-scale teleconnection patterns

Cătălin-Constantin Roibu[1] · Viorica Nagavciuc[1,2] · Monica Ionita[2] · Ionel Popa[1,3,4] · Sergiu-Andrei Horodnic[1] · Andrei Mursa[1] · Ulf Büntgen[5,6,7,8]

Received: 7 December 2020 / Accepted: 9 March 2022 / Published online: 31 March 2022

Abstract
We present a new beech (*Fagus sylvatica* L.) tree-ring width composite chronology from five natural low-elevation forests in eastern Romania, which represent the species' continental distribution limit. Our regional beech chronology reflects April–June hydroclimate variability in form of the Standardized Precipitation Evapotranspiration Index over large parts of Romania, Ukraine, and the Republic of Moldova, for which high-resolution paleoclimatic evidence is broadly missing. Most of the reconstructed hydroclimatic extremes back to 1768 CE are confirmed by documentary evidences, and a robust association is found with large-scale atmospheric circulation patterns in the Northern Hemisphere and sea surface temperatures over the North Atlantic. Reconstructed pluvials coincide with a high-pressure system over the North Atlantic Ocean and north-western Europe, and with a low-pressure system over south-western, central and eastern Europe, whereas historical droughts coincide with a high-pressure system over Europe and a low-pressure system over the central part of the Atlantic Ocean. Our study demonstrates the potential to produce well-replicated, multi-centennial beech chronologies for eastern Europe to reconstruct regional hydroclimate variation and better understand the causes and consequences of large-scale teleconnection patterns.

Keywords Climate reconstructions · Dendroclimatology · Drought extremes · Eastern Europe · Teleconnection patterns · Tree rings · Beech

1 Introduction

The first two decades of the twenty-first century were characterized by a record number of climate extremes and climate-related disasters in different parts of the globe, which strongly affected socio-economic development (IPCC 2018). In a world with more frequent and more intense climate extremes combined with a fast-growing population, the costs of climate change impact will reach up to hundreds of billions of euros every year, causing irreversible damage to the natural environment, with serious consequences for biodiversity and society. With this in mind, relevant adaptive measures aimed to mitigate climate change impacts, become crucial for economic growth, durable management of food and water resources, ecosystem protection, and biodiversity conservation. Proper strategies need to be designed to preserve and assure ecosystem functions for future generations. In this respect, the scientific community plays a key role in delivering accurate and relevant predictions that can ensure a solid base on which suitable policies will be initiated.

✉ Viorica Nagavciuc
nagavciuc.viorica@gmail.com

[1] Forest Biometrics Laboratory, Faculty of Forestry, "Stefan Cel Mare" University of Suceava, Universității Street No. 13, 720229 Suceava, Romania

[2] Alfred Wegener Institute for Polar and Marine Research, Bussestr. 24, 27570 Bremerhaven, Germany

[3] National Research and Development Institute for Silviculture "Marin Drăcea", Calea Bucovinei No. 76bis, 725100 Câmpulung Moldovenesc, Romania

[4] Center of Mountain Economy, INCE-CE-MONT Vatra Dornei, Petreni Street No 49, 725700 Vatra Dornei, Romania

[5] Department of Geography, University of Cambridge, Cambridge CB2 3EN, UK

[6] Swiss Federal Research Institute (WSL), 8903 Birmensdorf, Switzerland

[7] Global Change Research Centre (CzechGlobe), 60300 Brno, Czech Republic

[8] Department of Geography, Faculty of Science, Masaryk University, 61300 Brno, Czech Republic

For the eastern part of Romania, climate change scenarios show an increase in the frequency and intensity of summer droughts over the next decades (Busuioc et al. 2010). As drought extremes are expected to intensify in terms of severity and extent, agriculture and forest ecosystems will face greater threats with a significant impact on the Romanian economy and society. In the last few decades, major efforts were made to study current and past climatic variations to develop more accurate climate models to improve forecast precision. The accuracy of climate models depends on the resolution of the input data, and from the natural proxy archives, tree rings are one of the most valuable, due to their annual resolution and precise dating. Tree-ring parameters, such as ring width, wood density, and stable isotopes, measured in different species and sites, from temperate and boreal zones, are used to develop long chronologies, representing the support on which different climate variables can be reconstructed (Fritts 1976). At the European level several reconstructions exist for hydroclimate, mainly focusing on the western and central part of Europe (Brázdil et al. 2002; Masson-Delmotte et al. 2005; Cufar et al. 2008; Haneca et al. 2009; Büntgen et al. 2010; Kress et al. 2010; Cook et al. 2015; Helama et al. 2018), while for the eastern part of the continent, only a few regional dendro-based climate reconstructions are available (Köse et al. 2013; Levanič et al. 2013; Nagavciuc et al. 2019a).

Most of the long tree-ring width chronologies were built using species belonging to *Pinus* and *Picea* genus, which account together for more than half of the International Tree-Ring Data Bank datasets, followed by *Quercus* species which account for almost a quarter of them (Zhao et al. 2019). The high number of chronologies from coniferous species can be explained by their natural distribution, usually at high latitude/elevation, where the level of sensitivity to climate conditions and variability is most pronounced. On the other hand, deciduous tree species are usually distributed at lower latitudes/elevations, where climate conditions do not always have such a strong influence on the growth process and dendroclimatic studies are less suitable in these areas, but their potential remains unexplored.

Despite the efforts made so far, the distribution of climate reconstructions is uneven and some important regions remained a knowledge gap regarding the past spatio-temporal climate variability. For example, for western and central Europe and the Mediterranean region, several long-term tree-ring paleoclimate reconstructions were developed, while the eastern part of Europe is less studied (Nagavciuc et al. 2020). In Romania, there are only a few tree ring-based reconstructions: three temperature reconstruction in the Eastern Carpathians (Popa and Cheval 2007; Popa and Kern 2009; Popa and Bouriaud 2013), and a drought reconstruction in the southern part of the country (Levanič et al. 2013), all based on coniferous species. The dendrochronological potential of beech (*Fagus sylvatica* L.) and oak (*Quercus*) at the eastern or southern limit of their natural distribution (Roibu et al. 2017, 2020, 2021), however, has not been considered in climatic reconstructions. Even though the large-scale drought reconstruction at the European level (OWDA and ERDA; Cook et al. 2015, 2020) covers the eastern part of Romania, the chronologies used inversely in the calibration models are coniferous species from the mountain region, being less sensitive to drought (Cook et al. 2015). Moreover, the OWDA or ERDA database for the eastern Carpathians region does not contain tree-ring data from low elevation sites or drought-sensitive species, being a gap of information that needs to be filled.

The presence of beech forests, with ages that reach ~ 300–400 years, in the north-eastern part of Romania and drought-sensitive sites, offer a unique possibility to test the usefulness of this species for climatic reconstructions, filling the knowledge gap in this area (Roibu et al. 2017). In this respect, the aim of this study is two-fold: (i) to explore the climate signal potential, recorded by interannual growth variability of beech (*Fagus sylvatica* L.) from the ecotone region, for paleoclimate reconstruction and (ii) to reconstruct the hydroclimatic variability over the last two and a half centuries in the north-eastern part of Romania. We statistically analyze the spatial and temporal stability of the reconstructed hydroclimatic variability and investigate the link between its variability and large-scale atmospheric circulation.

2 Material and methods

2.1 Study area

The study area is located in the north-eastern part of Romania (Fig. 1), at the eastern limit of the beech natural distribution (von Wühlisch 2008). The landscape consists of plateaus and hills with elevations ranging from 210 to 490 m asl. The forest is dominated by European beech (*Fagus sylvatica* L.), which grows in pure stands on higher grounds and in a mixture with oak (*Quercus robur*) on the plateau. The soil is formed by argic horizons on the sedimentary deposit, with stratified texture in sandy and clay horizons. The local climate regime is temperate-continental, with hot and dry summers. The mean temperature over the analyzed region is 8.5 °C, with the maximum in July (19.4 °C) and minimum in January (−3.7 °C), and the mean precipitation amount is 540 mm/year, of which 75% is recorded from April to September, over the 1971–2000 period.

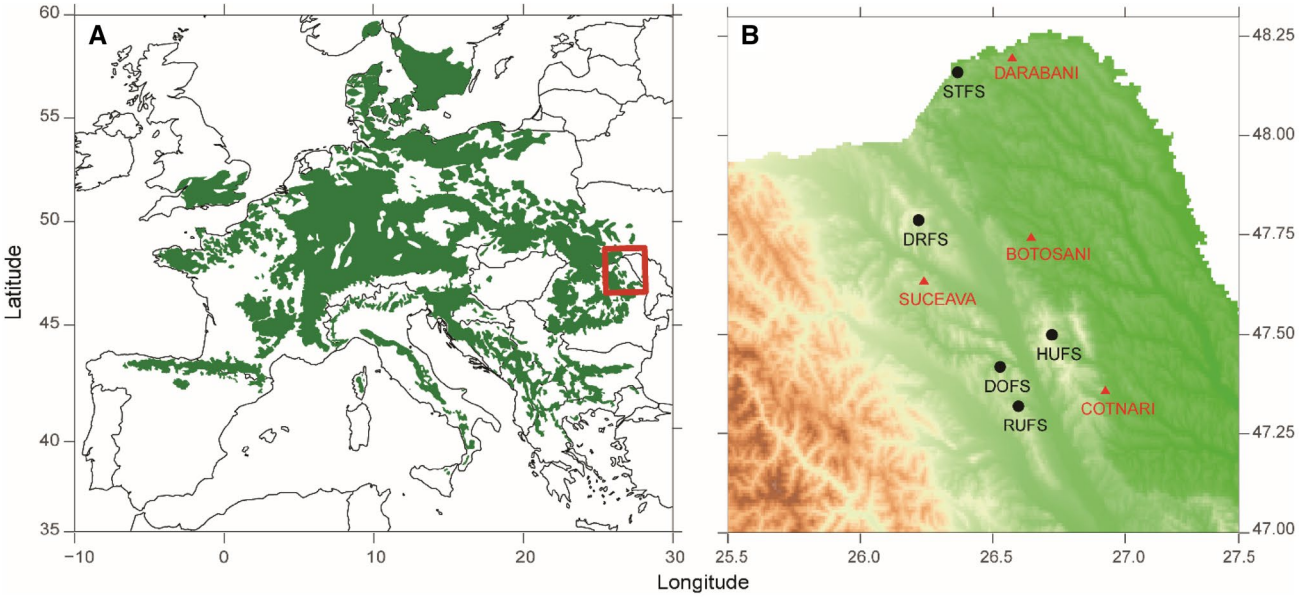

Fig. 1 Site location A: Site location in Europe—red square, with green is the distribution of the beech forests in Europe; B. Site location in the north-eastern part of Romania (red triangles—meteorological stations, black circles—sample sites, STFS—Stuhoasa, DRFS—Dragomira, HUFS—Humosu, RUFS—Ruja, DOFS—Dolhesti)

Table 1 Geographical features of the sampled beech sites and the replication for each site

Location	Code	Latitude (decimal degrees)	Longitude (decimal degrees)	Elevation (m a.s.l)	No. of trees sampled
Stuhoasa	STFS	48.15	26.36	210	39
Dragomirna	DRFS	47.42	26.52	330	39
Humosu	HUFS	47.49	26.72	350	30
Ruja	RUFS	47.31	26.59	360	16
Dolheşti	DOFS	47.79	26.22	490	58

2.2 Chronology development

The regional chronology was developed based on existing tree-ring width time-series from five representative beech forests from the north-eastern part of Romania (Fig. 1, Table 1). These tree-ring chronologies were part of a previous study marked as a plateau group (Roibu et al. 2017). More details about sampling, sample preparation, measurements, and cross dating are given in Roibu et al. 2017. Standard statistical parameters were computed for each tree-ring series (Fritts 1976; Cook and Kairiukstis 1990). Each raw series was transformed into a growth index by division using a cubic smoothing spline, with a 50% frequency response cut-off at 150 years (Cook and Kairiukstis 1990) in *dplR* package (Bunn 2008). The residual autocorrelation was removed using an autoregressive model. After testing the differences between individual site chronologies, the regional chronology was obtained by integrating all 182 tree-ring series, using the bi-weight robust mean (Fritts 1976; Cook and Peters 1997). The mean segment length (MSL) was evaluated after the age-aligning using their innermost ring (Fig. 2b).

The robustness of the obtained mean chronology was tested using expressed population signal (EPS) and subsample signal strength (SSS) (Wigley et al. 1984). The difference between these indices is that SSS estimates the loss explained variance of climate reconstruction back in time due to the decreasing of sample size, while EPS represents an indicator of the strength of the unknown population signal (Wigley et al. 1984; Buras 2017). Once transfer functions have successfully passed validation tests, SSS is the appropriate measure to estimate the loss of explanatory power due to a decreasing sample size back in time (Buras 2017). The minimum sample depth to ensure a strong common signal among trees was based on years when the SSS/EPS was greater than 0.85 (Briffa and Jones 1990). Also, the series confidence interval was tested using the inter-series correlation (Rbar) (Wigley et al. 1984) and NET index (Esper et al. 2001). Rbar estimates the common variance between single series, independent of the series number. The NET index was used to estimate the signal strength of mean tree-ring chronologies with annual resolution and it combines the coefficient of variation and the synchronicity. High NET index values indicate low signal strength of the chronology, and vice versa.

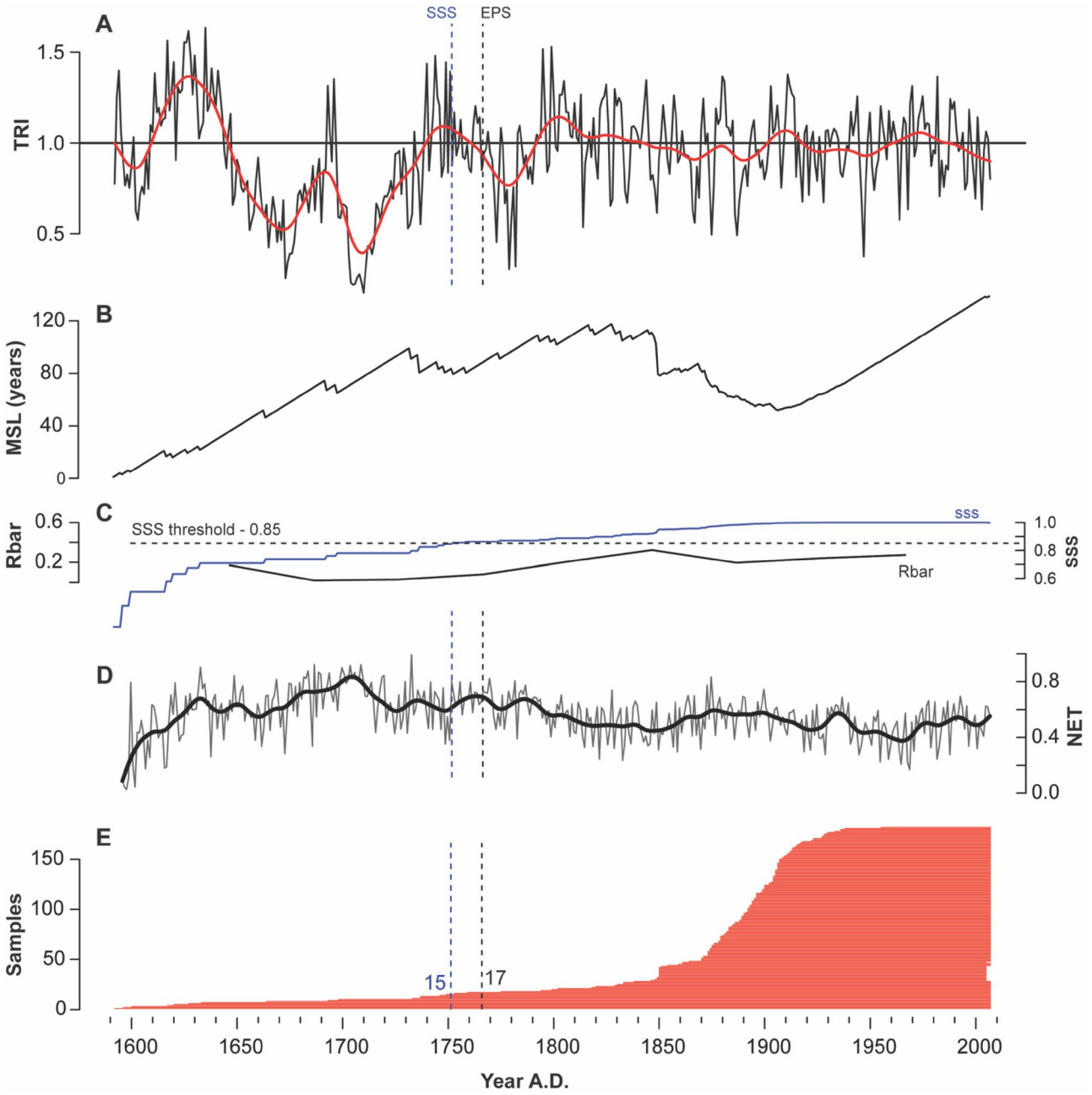

Fig. 2 Beech tree-ring width chronology from NE Romania and its signal strength statistics, **A** tree-ring width index (TRI), (black—residual values, red—low pass 32 yrs filter); **B** mean sample length (MSL); **C** subsample signal strength (SSS) and inter-series correlation (Rbar); **D** NET tree-ring index (grey -NET index, black line—low pass 20 yrs filter); **E** chronology sample depth; (blue and black dotted lines indicate periods with SSS, respectively EPS are greater than 0.85)

2.3 Climate data and drought reconstruction

Climate–growth relationship was assessed using mean temperature and precipitation amount obtained from CRU T.S. 4.04 gridded database, from the closest grid points to our study region (26.25–26.75° E/47.25–48.25° N) (Harris et al. 2020), for the 1901–2016 period. As both climatic parameters have a strong influence on tree growth (Roibu et al. 2017), we analyzed the relationship between the regional tree-ring chronology and a drought index. For this, we used the Standardized Precipitation and Evapotranspiration Index (SPEI), calculated for 3 months of accumulation period (SPEI3, from now on) (Vicente-Serrano et al. 2010). Pearson correlation analyses were performed with a monthly time window from June of the previous year to September current year of the growing season. The statistical significance

of the correlation was tested by the bootstrap method (Efron and Tibshirani 1986; Guiot 1991). The correlation analyses were performed using the *treeclim* package (Zang and Biondi 2015).

To test the spatial–temporal stability of the relationship between the TRW records and climate variables we also make use of stability maps, a methodology successfully applied in the seasonal forecast of the European rivers and Arctic sea ice, to examine the stationarity of the long-term relationship between our proxies and the gridded climate data (Ionita et al. 2008, 2019). Although this methodology is mostly used for forecast purposes, recently it has also been successfully applied in dendroclimatological studies (Nagavciuc et al. 2019b, 2020). In order to detect stable predictors, the variability of the correlation between the TRW time series and the gridded data is investigated within a 41-year moving window over the period from1901 to 2007. The analysis was performed for a time window that starts in September of the previous year, and ends in August of the current year. The correlation is considered stable for those regions where the TRW index and the gridded data (i.e. SPEI3) are significantly correlated at the 95%, 90%, 85% or 80% level for more than 80% of the 41-year moving windows. The first window is represented by the correlation between the TRW index and SPEI3 over the period 1902–1942, the second window is represented by the correlation between the TRW index and SPEI3 over the period 1902–1942, and so on until the last window which is represent by the correlation between the TRW index and SPEI3 over the period 1977–2007. For the current study only regions where the correlation is above 95% significance level, are retained for further analysis. A detailed description of the methodology is given by Ionita (2017). The basic idea of this methodology is to identify regions with stable correlations (meaning the correlation does not change over time) between the TRW index and gridded data (e.g. SPEI3) with different time lags.

The June SPEI3 drought reconstruction is based on a linear regression model. To estimate the reliability and predictive power of the reconstructed model we have split it into calibration and verification subsets of equal lengths, over the full period (1901–2007) (Cook et al. 1995; Meko and Graybill 1995). The reduction of error (RE), the coefficient of efficiency (CE), and the Durbin-Watson test (DW) were used to estimate the robustness of the regressive model. Taking into account that the regression-based reconstruction underestimates the reconstruction value variability when compared with the instrumental data, we rescaled the reconstructed values with the mean and standard deviation of instrumental SPEI values over the entire calibration interval (Esper et al. 2005).

Dry extreme events are defined as years when the SPEI3 index is smaller than -1.5, while wet extreme events are defined as years when the SPEI3 index is higher than + 1.5 (Vicente-Serrano et al. 2010). Additionally, we tested the occurrence of the extreme events variability from the reconstructed chronology with historical/documentary data sources, available for Romania (mainly focused on the Transylvania region), Moldova, and western Ukraine. The documentary sources reflect periods of warm/cold, dry/wet episodes, floods, droughts or fires, which affected agricultural production, such as poor grains, crops, hay richness, etc. with direct implication on food production and/or famine. The temporal evolution of hydroclimate changes in the last two and a half centuries was analyzed by applying the probability density function for five different periods, each of 50 years.

Moreover, to assess the regional hydro-climatic signal in eastern Europe, we compared our reconstruction with other five reconstructions available from the eastern and southern part of Europe: Slovakia (Büntgen et al. 2010), Crimea (Solomina et al. 2005), north-eastern Hungary (Kern et al. 2013), north Aegean (Griggs et al. 2007) and south-western Romania (Levanič et al. 2013). These comparisons were made between original (unfiltered) and smoothed data (20 years low pass filtering). Significance levels of the smoothed timeseries were corrected for lag-1 autocorrelation using a frequency-domain method (Ebisuzaki 1997).

2.4 Composite maps

To investigate the link between the East Romanian early summer drought variability and the large-scale atmospheric circulation patterns we used the seasonal means of Geopotential Height at 500 millibars (mb) (Z500), zonal wind (U500), and meridional wind (V500) at 500 mb from the Twentieth Century Reanalysis (V2) data set (Whitaker et al. 2004; Compo et al. 2006, 2011) on a $2° \times 2°$ grid, over the period from 1860 to 2007. For the Sea Surface Temperature (SST) we used the $1° \times 1°$ Hadley Centre Sea Ice and Sea Surface Temperature data set—HadISST (Rayner et al. 2003). These data sets have global coverage.

To identify connections with the large-scale atmospheric circulation and the North Atlantic Ocean SST, we constructed the composite maps of Z500 and SST standardized anomalies for the late spring season (April–May–June) by selecting the years when the value of the normalized TRW time series was > 1 standard deviation (High) and < -1 standard deviation (Low), respectively. This threshold was chosen as a compromise between the strength of the climate anomalies associated with the TRW anomalies and the number of maps that satisfy this criterion. Further analysis has shown that the results are not sensitive to the exact threshold value used for the composite analysis (not shown). The significance of the composite maps is based on a standard t-test (confidence level 95%).

3 Results and discussions

3.1 Chronology characteristics

The regional beech chronology was developed based on five local chronologies from the eastern limit of the natural distribution of beech forests in Europe (Fig. 1, Table1), and covers the period from 1592 to 2007 (Fig. 2a). The mean tree-ring width is 1.99 ± 0.98 mm, and the average age obtained for most of the analyzed period is 80 years, except the twentieth century where the MSL reach 140 years (Fig. 2b). The mean sensitivity of the tree's reaction to environmental changes is 0.35 (0.2–0.5) and the first-order autocorrelation for raw data (AC1) is 0.63. The correlation between local chronologies ranges from 0.354 ($p < 0.001$) to 0.746 ($p < 0.001$), and the mean inter-series correlation of the regional chronology is 0.503 ($p < 0.001$). The high value of the first principal component (PC1, 61.02%) indicates a strong influence of one factor (probably a climate factor) on tree-ring width variability. This result is strengthened by the high value (86.14) of the signal to noise ratio (SNR).

The EPS threshold, above 0.85, is reached after the year 1767 with a replication of 17 samples, while the SSS threshold is reached after 1752 with a replication of 15 samples. For these reasons, further analyses are limited to the period 1767–2007. The NET index shows a good temporal signal strength of tree ring chronology after 1760 (Fig. 2). The narrowest rings were registered in 1782, 1779, 1875, 1887, 1947, and 1964, and the widest rings were registered in 1799, 1795, 1844, 1911, 1970, and 1982.

3.2 Climate–growth relationship

Exploratory data analysis shows a significant positive correlation between the regional tree-ring width index and precipitation amount from April ($r = 0.33$), and May ($r = 0.34$), and a significant negative correlation with mean June temperature ($r = -0.43$) (Table 2). These findings support the statement that, in Eastern Europe, there is a significant correlation between beech radial growth and summer drought (Roibu et al. 2017; Garamszegi et al. 2020).

According to obtained stability maps (Fig. 3) and correlation map (Figure S1), the correlation between TRW and SPEI3 is positive, stable, and significant in September previous year, over the eastern part of Romania, the Republic of Moldova, and western part of Ukraine, in May over the southeastern part of Romania and the Republic of Moldova, in June over Romania, the Republic of Moldova, and Ukraine, and in July over Romania, and western Ukraine (Fig. 3). This high, significant, and stable correlation indicates that the beech TRW indices from north-eastern Romania register both local as well as regional-scale drought variability. For the reconstruction analysis, we have defined a SPEI3 index for June based on the stability map, by averaging the gridded data sets over the region 45–51.5° N, 23.5–31°E, which represents the area with the stable and significant correlations (the black box in Fig. 3).

TRW also shows a significant correlation with the SPEI3 drought index (defined also as an average over the region 45–51.5° N, 23.5–31° E) from the spring and summer months (from May to August), with the highest correlation coefficient for June ($r = 0.51$) (Fig. 4A). In addition, a significant correlation was found between TRW and July, August, and September SPEI3 of the previous year. The correlation with June SPEI 3 could be related to the cambial activity which is strongly influenced by water deficits, which have a direct implication on the number of xylem cells produced, the xylem-phloem proportion and earlywood–latewood relation (Pallardy 2008). Spring and summer water deficit inhibits the cambial activity, which slows and/or ceases the xylem development, resulting in a narrow tree ring width, during the dry years, while water availability stimulates tree growth, resulting in a wider tree ring (Kozlowski and Pallardy 1997). The previous year's climatic conditions can influence the current year's growth via carbohydrates accumulation and hormonal growth regulators which are affected by water availability from the previous year (Pallardy 2008).

The positive values of RE and CE, for both forward and reverse models, indicate good reconstruction skills (Table 3, Fig. 4B). The DW values are close to 2 suggesting no autocorrelation. For the final regression model, we used the full 1902–2007 period to develop a June SPEI3 drought reconstruction (Table 3), reaching back to 1768,

Table 2 Correlation coefficients of tree-ring width and monthly climatic data: precipitation (Prec), mean temperature (Temp), and SPEI3 drought index, from June previous year to September current year and April/May (AM) and May/June/July (MJJ) periods, with blue-highlighted/bold are significant ($p < 0.05$) negative correlation and with bold-highlighted/red significant positive correlations

	jun	jul	aug	sep	oct	nov	dec	JAN	FEB	MAR	APR	MAY	JUN	JUL	AUG	SEP	AM	MJJ
Prec	0.15	0.22	0.06	0.20	-0.02	0.14	0.07	0.00	-0.14	0.01	**0.33**	**0.34**	0.13	0.15	-0.11	0.00	**0.45**	**0.33**
Temp	-0.22	**-0.39**	-0.29	-0.30	0.04	0.00	0.23	0.00	0.10	0.14	-0.22	-0.21	**-0.43**	-0.22	-0.15	-0.13	**-0.30**	**-0.41**
SPEI3	0.25	**0.39**	**0.33**	**0.38**	0.20	0.22	0.15	0.13	-0.03	-0.10	0.15	**0.37**	**0.51**	**0.44**	0.28	0.09		

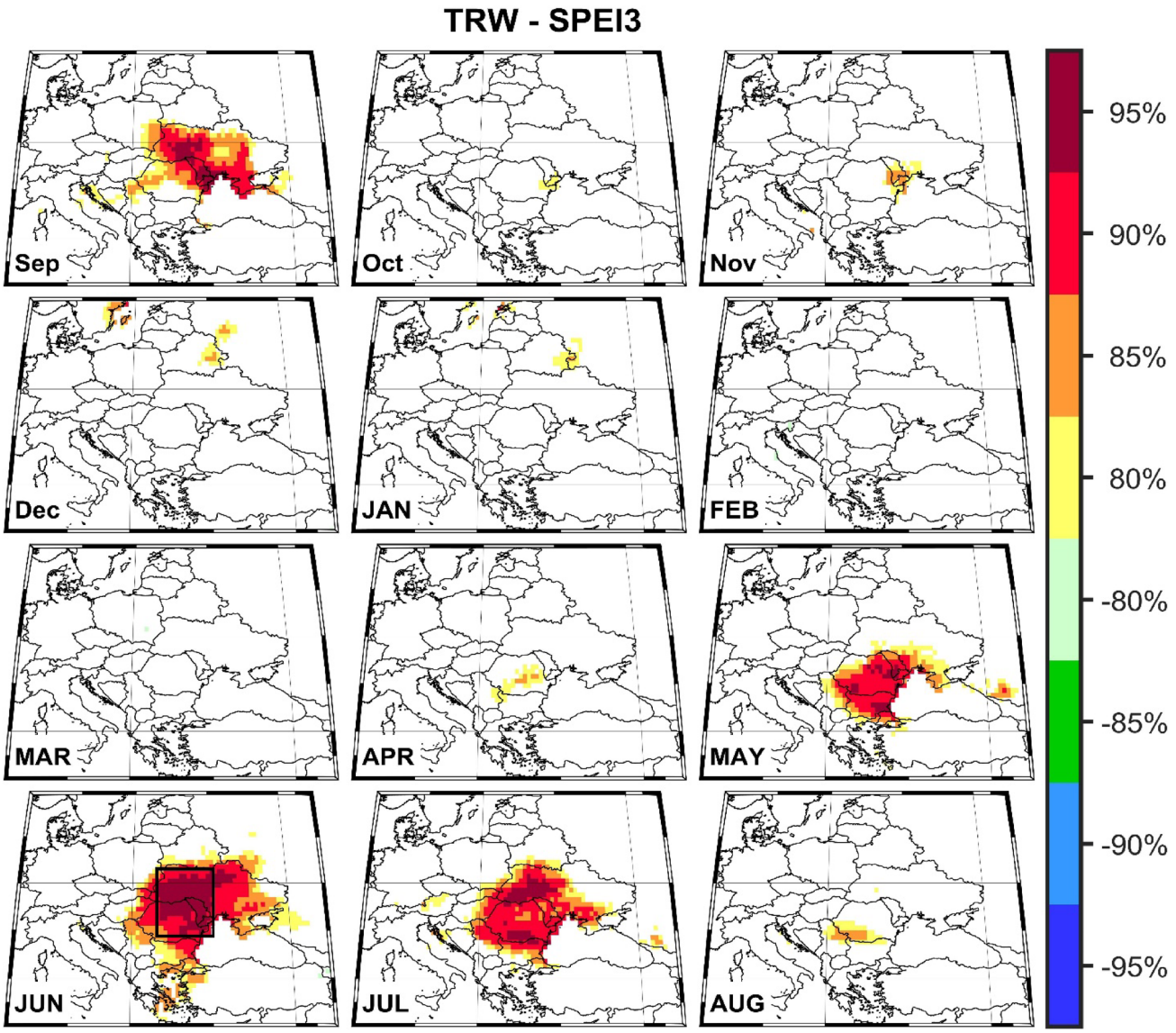

Fig. 3 Stability map of the correlation between TRW and SPEI3 from previous year September until current year August. Regions where the correlation is stable, positive, and significant for at least 80% windows are shaded with dark red (95%), red (90%), orange (85%), and yellow (80%). The corresponding regions where the correlation is stable, but negative, are shaded with a dark blue (95%), blue (90%), green (85%), and light green (80%). Sep—September previous year, Oct—October previous year, Nov—November previous year, Dec—December previous year, JAN—January, FEB—February, MAR—March, APR—April, MAY—May, JUN—June, JUL—July and AUG—August. Analyzed period: 1902–2007. The significance level is computed based on a two-tailed *t*-test

where the chronology meets the EPS threshold. Our reconstruction skills are in line with other hydro-climatic reconstructions based on tree-rings width (Akkemik et al. 2005; Büntgen et al. 2010; Levanič et al. 2013).

3.3 Drought reconstruction

Here we present the first drought reconstruction for eastern Europe, back to 1768 based on tree-rings width of 182 living beech (Fig. 5). The June SPEI3 reconstruction preserves inter-annual to inter-decadal variations over the analyzed period. In the last 239 years, the wettest periods occurred in the following intervals: ~ 1795–1813, ~ 1903–1914,

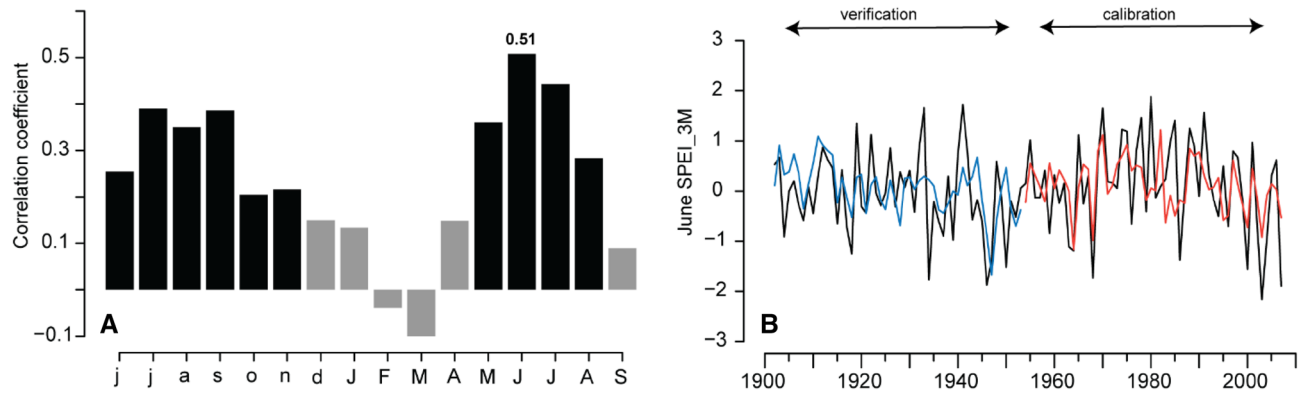

Fig. 4 **A** Correlation coefficient between tree-ring width index and SPEI3 (grey bars—insignificant correlation, black bars—significant correlation); **B** calibration-verification model for June SPEI3, black line—observed data, red and blue line—reconstructed June SPEI3 for calibration and verification periods respectively

Table 3 Summary table of calibration and verification statistics of June SPEI3 reconstruction

Sub-period	r^2	r	RMSE	DW	RE	CE
Early calibration (1902–1953)/late verification (1954–2007)	0.19	0.43	0.12	2.07	0.28	0.26
Early verification (1902–1953)/late calibration (1954–2007)	0.30	0.55	0.12	2.25	0.17	0.13
Full calibration period (1902–2007)	0.26	0.51	0.75	2.08	–	–

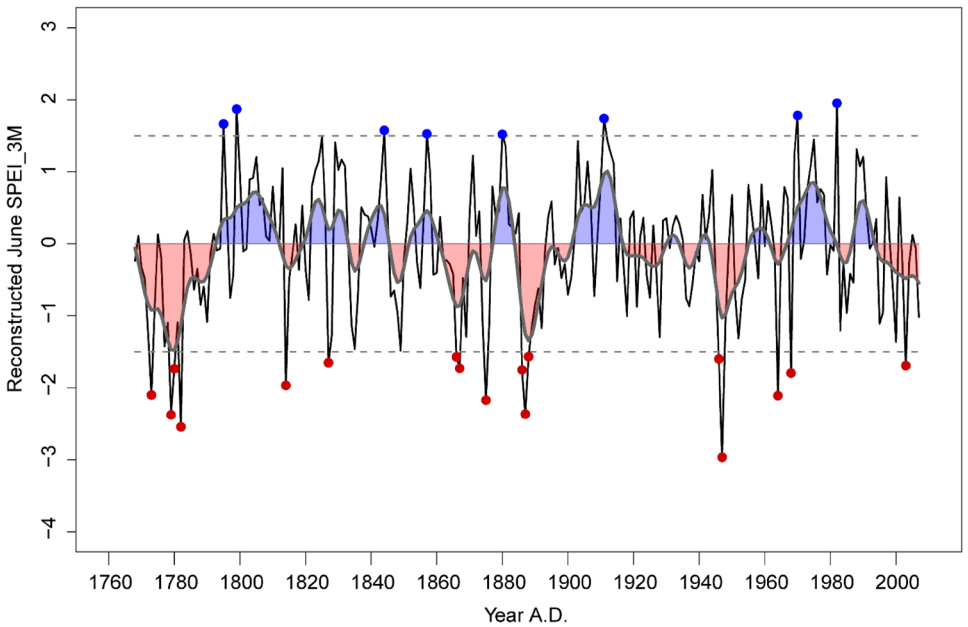

Fig. 5 The rescaled reconstructed June SPEI3 drought index for the 1768–2007 period. The gray line represents a 11-yr low-pass filter and the dashed lines depict (extreme events threshold detection) ± 1.5 SPEI threshold, while the values above/below dashed line corresponds to very wet/dry years (additionally marked with blue and red dots)

and ~ 1969–1982, while the driest ones prevailed in the: ~ 1770–1790, ~ 1885–1900, ~ 1945–1968, and after ~ 1990. A total number of 25 extreme events were identified in our reconstruction (17 extreme dry events and only 8 extreme wet events). The wettest April–June period was recorded in 1982 (+ 1.95), while the driest one was in 1947 (−2.57). The number of extremely dry years and their distribution along the reconstruction period differ significantly from the number and distribution of wet years. Five of the eight extreme positive years were identified between 1795 and 1880, another one at the beginning of the twentieth century (1911), and the other two between 1970 and 1982. In the eighteenth century were recorded four extreme dry years, during the nineteenth century eight extreme dry years, while in the twentieth century were recorded five extreme dry years. Consecutive years with extreme dry spring to

summer seasons were identified in 1779–1780, 1866–1867, 1946–1947 (two consecutive years), and 1886–1888 (three consecutive years). No consecutive years with extreme wet spring to summer seasons were revealed by our reconstruction.

In order to identify the statistical temporal distribution of hydroclimate changes over the last two and a half centuries, we split our June SPEI3 drought reconstruction into five periods of 50 years (Fig. 6). The probability distribution functions of all five periods are normally distributed and indicate a similar occurrence of the dry and wet events. However, these probability density functions present different variance levels: low variance during the 1768–1820, 1871–1920, and 1921–1970 periods; high variance in the 1821–1870 period, while between 1971 and 2007 the probability distribution function presents a medium variance. Comparing the shape of the five distributions, the 1821–1870 and 1971–2007 periods stand out with distinct and significant differences ($p < 0.005$, based on Kolmogorov–Smirnov two-sample test). These findings indicate a change in the climatic regimes, which caused an increasing frequency of extreme events. Moreover, for the period from 1971 to 2007, these changes can also be easily observed in the chronology trend.

To check the occurrence of the extreme events on our reconstruction before the beginning of the instrumental records, in our case 1961, when the national meteorological network was established in Romania, we made use of different historical/documentary sources. We found documentary sources that confirm all 25 extreme events identified by our June SPEI3 drought reconstruction (Table 4). The extreme events, both dry and wet spells, are mentioned in historical archives as catastrophic events with a high impact on the lives of the inhabitants, especially through agricultural production and socio-economic development. Among the most used short descriptions of extreme events in the historical archives are big floods or droughts with a negative impact on human lives and crops and food production, famine, lack of animal feed, drying wells, disease, extreme frost, etc. For example, the extremely dry years of 1946 and 1947 were mentioned as "warm and extremely dry spring and summer" with very poor crops, 1947 being also known in Romanian history as "the year with the greatest famine and poverty" (Topor 1963). 1827 was also recorded as a year with extreme drought, forest fire and very dry summer in Transylvania (Dudaș 1999), and 1887 as a year with very dry spring (Topor 1963; Mihailescu 2004). The extreme wet spells were also reported in the historical data: 1799 was described as a year with late spring and very cold winter, while the year 1844 was characterized by a cold and wet April and wet summer (Mihailescu 2004). For the more recent periods, the description of historical climatic records became more generous, containing more detailed information about those events. For example, in 1970 one of the biggest floods was recorded, affecting more than 1500 settlements, and more than one million hectares of land. As a result, 56 people and more than 20,000 animals died, and the economic costs were huge (AGERPRES 2020). Another example can be the drought in 2003, one of the driest and hottest summer at the European level, which marks the beginning of a series of extreme years (e.g. 2010, 2015, 2018) that occurred in the twenty-first century (Bakke et al. 2020; Ionita and Nagavciuc 2020, 2021). The drought of 2003 severely affected agriculture reducing annual crop productivity by up to 30% through premature ripening, drought-induced pest infestations, or diseases, diminished crop quality, and crop failure due to dieback (EDC 2013). Overall, the results of the calibration/verification test are confirmed by the good match of extreme years as recorded by our reconstruction with historical sources, which validate the robustness of our June SPEI3 reconstruction for the last two and a half centuries.

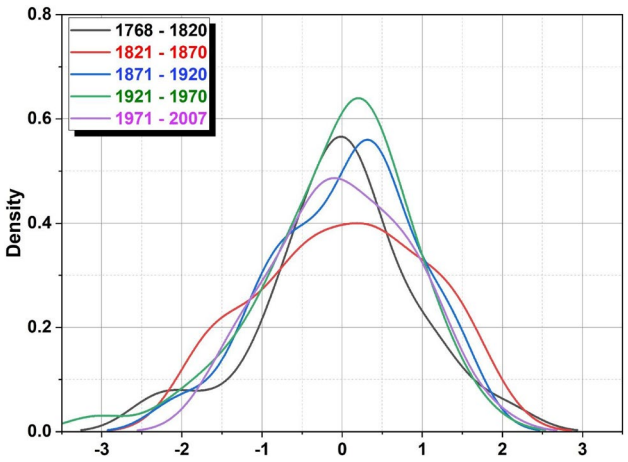

Fig. 6 The fitted distribution of the June SPEI3 values for different time-periods: 1768–1820 (black line), 1821–1870 (red line), 1871–1920 (blue line), 1921–1970 (green line), and 1971–2007 (pink line) for the reconstructed data

3.4 Large-scale atmospheric circulation

The intensity, duration, and interannual to multidecadal variability of drought and pluvial events are influenced by climatic factors (e.g. precipitation, temperature, soil moisture) as well as by the prevailing large-scale atmospheric circulation and the sea surface temperature (SST) (Ionita et al. 2012, 2015). Usually, anticyclonic (cyclonic) circulation during the spring and summer determines dry (wet) climatic conditions (Ionita 2015), which have a direct impact on tree-ring growth. The significant and stable correlation over the large area in the eastern part of Europe (Fig. 4) indicates that the developed beech TRW chronology reflects April–June drought variability at the eastern European scale,

Table 4 The occurrence of the extreme events from our June SPEI3 reconstruction in different historical/documentary sources over the analyzed area

	Year	May SPEI3	Documentary information
Wet spells	1795	1.66	The snow was as high as the house, one of the most extreme wet year in the western Hungary (Kern et al. 2009) (Dudaș 1999)
	1799	1.87	Late spring, very cold winter (Mihailescu 2004)
	1844	1.58	Cold and wet April in Ukraine, wet summer (Mihailescu 2004)
	1880	1.53	Rainy year, floods in Romania with 215 fatal victims (Teodoreanu 2017)
	1911	1.52	Excess rainfall and cold summer in Basarabia and Ukraine (Mihailescu 2004)
	1970	1.74	The worst floods in the history of Romania (AGERPRES 2020)
	1982	1.78	Rainy weather; cold spring (Mihailescu 2004)
Dry spells	1773	−2.10	Epidemic in south-western Russia (Mihailescu 2004)
	1779	−2.37	Drought and famine in Ukraine, one of the most extreme dry year in the western Hungary (Kern et al. 2009) (Mihailescu 2004; Teodoreanu 2017)
	1780	−1.73	Dry May (Topor 1963) (Dudaș 1999)
	1782	−2.54	A year with drought in the Western part of the Black Sea and as well as "the year with the extremely low water level in Danube river due to long period drought" (Büntgen et al. 2010)
	1814	−1.96	The great famine in Transylvania, In Vienna, large quantities of grain damaged by the rains were thrown into the Danube (Ciorba 2015)
	1827	−1.65	Very dry summer in Transylvania, forest fire (Dudaș 1999)
	1866	−1.57	Drought from June to September; 1865-drought in autumn (Topor 1963)
	1867	−1.73	Extreme dry spring; in Odesa 40 days of drought, insects, and drought in Basarabia, Podolia; storms and strong winds (Topor 1963; Mihailescu 2004)
	1875	−2.17	Dry spring; dry autumn; winter with less snow, summer without rain, rainy autumn in Ukraine, drought until June in Orhei (Moldova) (Mihailescu 2004; Teodoreanu 2017)
	1886	−1.75	Dry spring in Odesa, locust in Basarabia (Mihailescu 2004); dry year (Dudaș 1999)
	1887	−2.36	The entire spring was dry (Topor 1963)
	1888	−1.57	Very dry summer in Timiș, very low streamflow (Dudaș 1999)
	1946	−1.60	Warm and extreme dry spring; warm and very weather (Topor 1963; Mihailescu 2004; Teodoreanu 2017)
	1947	−2.97	Warm and extreme dry spring, spring was excessively dry (Topor 1963; Teodoreanu 2017)
	1964	−2.11	The severe drought in Romania (Ionita et al. 2015)
	1968	−1.79	Cyclone over the Adriatic Sea which brought snowstorms in the southeast of Europe (Mihailescu 2004)
	2003	−1.69	Very dry and warm year, extreme dry year in Romania (Ionita et al. 2015)

indicating that the TRW index variability is influenced by the large-scale atmospheric circulation. Thus, to explore the relationship between the beech TRW index from eastern Romania and large-scale atmospheric circulation we generate the composite maps using April–June (AMJ) northern hemisphere geopotential height at 500 mb (Z500) and the North Atlantic Ocean Sea Surface Temperature (SST) (Fig. 7, Table 5). For the high composite maps, we used the years when the TRW index was higher than 1 standard deviation (SD), and for low composite maps we used the years when the TRW index was lower than −1 standard deviation (SD). High values of beech TRW index are associated with a high-pressure system over the northern Atlantic Ocean and north-western Europe, and with a low-pressure system over the south-western, central, and eastern Europe (Fig. 7a). This pattern of the atmospheric circulation favors the advection of the wet and cold air from the north towards the central part of Europe, including our study site, which in turn leads to positive precipitation anomalies and low temperatures. Low values of the TRW index are associated with a high-pressure system over Europe and a low-pressure system over the central part of the Atlantic Ocean. This type of atmospheric circulation determines the advection of the dry and warm air from the south, which generates dry events over our study area. The obtained link between the beech TRW index and drought variability for the analyzed area is in concordance with the results reported by Ionita (2015), which has shown that the large-scale atmospheric circulation has a significant impact on the spring and summer climate variability over Europe, including Romania.

Next to the prevailing large-scale atmospheric circulation, the North Atlantic Ocean SST was found to have also a significant influence on the hydroclimate variability over Europe. Previous studies have shown the SST role in the interannual to decadal climate variability, as well as its influence on the occurrence of extreme climatic events

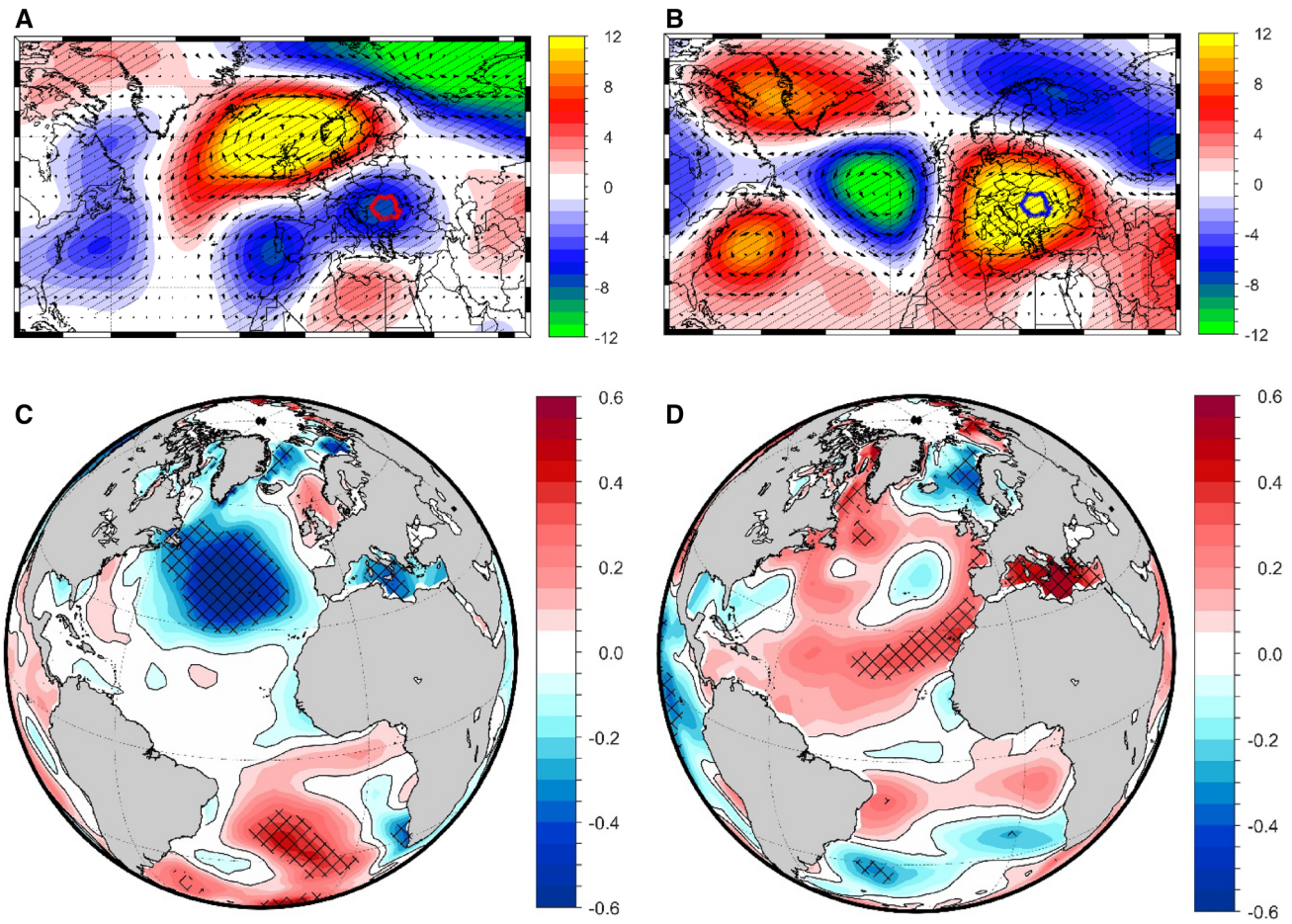

Fig. 7 **a** The composite map between high TRW index (> 1 SD) and April/May/June (AMJ) Geopotential height at 500 mb (Z500—Shaded colored areas) and AMJ 500 mb wind vectors (black arrows); **b** the composite map between low TRW index (<−1 SD) and AMJ geopotential height at 500 mb (Z500—Shaded areas) and AMJ 500 mb wind vectors; (**c**) as in (**a**) but for the AMJ sea surface temperature (SST) and (**d**) as in (**b**) but for the AMJ sea surface temperature (SST). The hatching highlights significant values at a confidence level of 95%. Analyzed period: Z500: 1836–2007, SST: 1854–2007. Units: Z (m) and SST (°C)

Table 5 The years corresponding to the high TRW values (> 1 SD) and low TRW values (< −1 SD) used for the Z500 and SST (with asterisks*) composite map analysis in Fig. 7. Analyzed period: Z500: 1836–2007, SST: 1854–2007

High TRW	Low TRW
1843, 1844, 1852, 1857*, 1858*, 1871*, 1880*, 1881*, 1903*, 1906*, 1911*, 1912*, 1913*, 1914*, 1944*, 1969*, 1970*, 1974*, 1975*, 1982*, 1988*, 1989*, 1990*, 1997*	1848, 1849, 1866*, 1867*, 1869*, 1874*, 1875*, 1876*, 1886*, 1887*, 1888*, 1889*, 1892*, 1918*, 1928*, 1946*, 1947*, 1948*, 1952*, 1964*, 1968*, 1983*, 1985*, 1995*, 1996*, 2000*, 2003*, 2007*

like droughts, heat waves, or floods in Europe (Ionita et al. 2012, 2021). Through a strong influence on climate variability, SST has also a significant influence on tree-ring growth, and has been previously used in dendrochronological studies (Nagavciuc et al. 2019a, 2020). Based on the composite maps between the TRW index and the North Atlantic basin SST we found that high values of the TRW index are associated with negative SST anomalies in the central and northern Atlantic Ocean, while the low TRW values are associated with positive anomalies over the Mediterranean Sea and western coast of Africa and southern Europe. The obtained results are confirmed by the link between positive anomalies of the Mediterranean SST and the occurrence of extreme drought events over the southern and eastern parts of Europe, including our study site (Van Lanen et al. 2016; Ionita 2017).

3.5 Comparison of the June SPEI3 drought reconstructions with other records

The new reconstructed June SPEI3 drought index was compared with the other five reconstructions available from central and south-Eastern Europe to assess their spatial synchronicity (Figs. 8, 9). The selected reconstructions used for these analyses reflect seasonal precipitation or drought variability between March and August. The results showed that our reconstruction retains both high and low-frequency variability similar to other reconstructions; however, their synchronicity is not stable in time. The high-frequency similarities are expressed through the extreme years registered by different reconstructions. For example, an extremely dry year recorded in 1782 is also mentioned as "the year with drought in the western Black Sea" by Akkemik et al. (2005) and "the year with the extremely low water level in Danube river due to long period drought" by Büntgen et al. (2010). Other extreme dry years that have been mentioned in other reconstructions are 1779 in Bohemia (Dobrovolný et al. 2018) and western Hungary (Kern et al. 2009), 1875—in eastern Mediterranean (Griggs et al. 2014), western Black

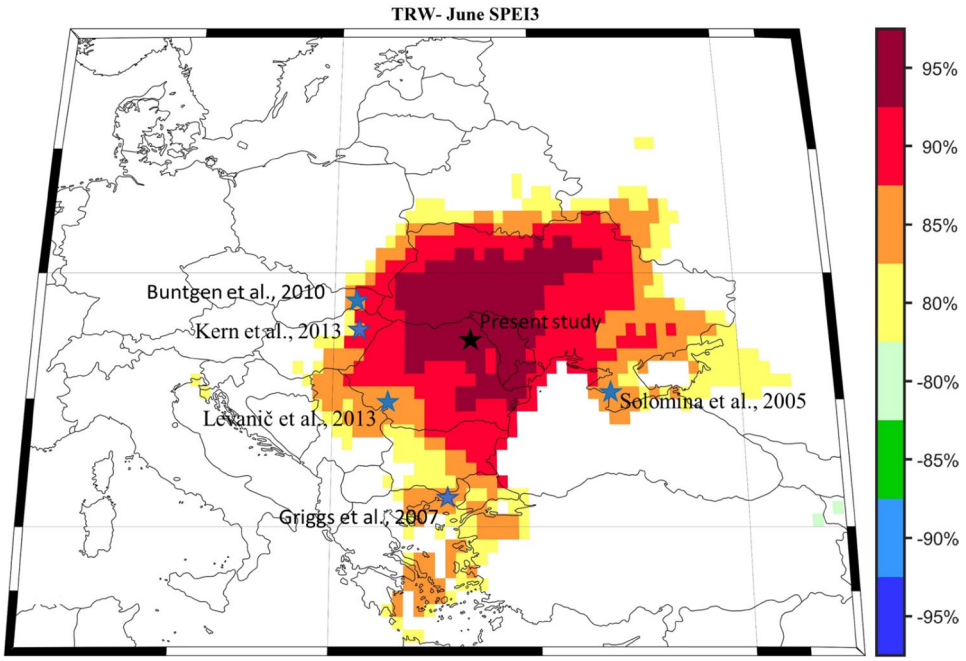

Fig. 8 The stability map of the correlation between TRW and SPEI3 for June (see Fig. 3) and the locations of different reconstructions used for comparison with our reconstruction (see Fig. 9). The blue stars are indicated the location of the other reconstructions used in Fig. 9 or Table 5, and black star indicated the present study location

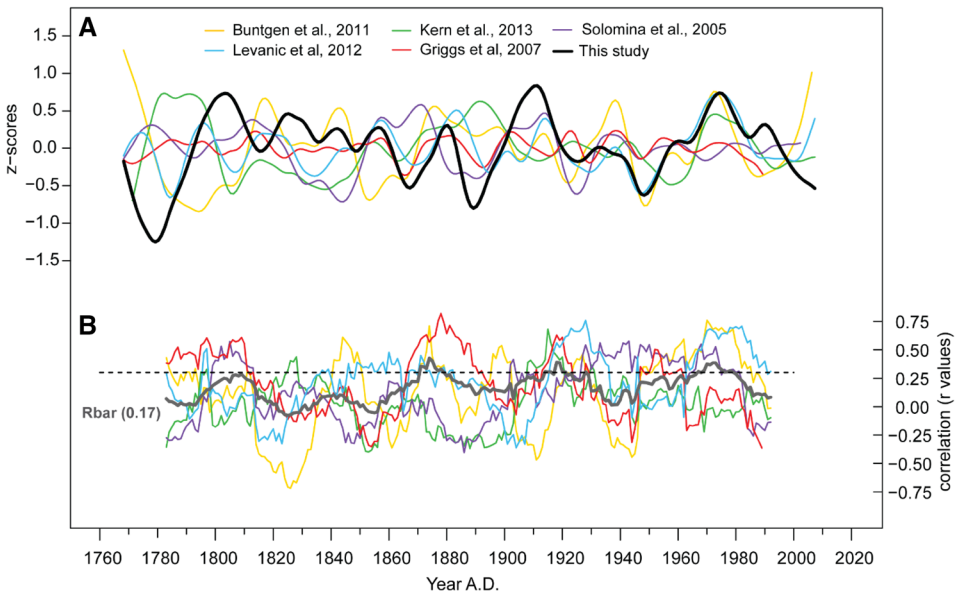

Fig. 9 Comparison with other hydroclimatic records from central and south-eastern Europe, **A** low-frequency variability—each curve represents a 21-yr. low-pass filter; **B** A 31 yrs. moving correlation between this study and five hydroclimatic raw data records (dotted line marks the positive correlation significance level at $p < 0.05$, the grey line is the mean inter-series correlation (Rbar) between all individual hydroclimatic records over 31 year moving windows

Sea (Akkemik et al. 2005), and in eastern Russia (Cook et al. 2020), 1887—in the Czech Republic (Büntgen et al. 2011) and Anatolia (Touchan et al. 2007), and 1947—in Slovakia (Büntgen et al. 2010), southern-western Romania (Levanič et al. 2013) and north Aegean Sea (Griggs et al. 2007). Among the extreme wet years, we identified only one common year, 1970, in Slovakia (Büntgen et al. 2010).

In the low-frequency domain, a comparison between our reconstruction and the other five records shows similar features, pinpointing a regional extension of some of the extreme events (Fig. 9A). A higher correlation coefficient, after 21-year low-pass filtering, is found between our reconstruction and summer drought index from southern-western Romania ($r=0.40$) (Levanič et al. 2013). Furthermore, a good correlation, but without statistical significance, was found with spring precipitation from the Western Black Sea ($r=0.22$) (Akkemik et al. 2005), and May–June precipitation from the southwestern Black Sea ($r=0.23$) (Griggs et al. 2007) (Fig. 9A, Table 6). However, the synchronicity is not stable in time; higher correlations were found for the nineteenth century than for the eighteenth century (Table 6). These low and unstable correlations can be mainly explained by a series of different factors, such as: the distance between the compared reconstructions, species used (oak, pine, silver fir), reconstructed parameters (e.g. precipitation, scPDSI, SPI), or seasonal response window selected (from March to August). In addition, the selected reconstructions are coming from areas for which the June SPEI3 drought signal recorded by the beech tree-ring from northeastern Romania is unstable or at the limit of this area, except for the reconstitution by Levanič et al. (2013), with which we obtained the highest correlations (Fig. 8). Running 31-year correlations among the individual time series and their averages (*Rbar*) have shown that higher correlations appeared over 1820–1840 and 1870–1930 (Fig. 9B).

3.6 Sources of uncertainty

An important aspect of climatology is the availability of reliable and continuous data and their accurate interpretation (Büntgen et al. 2011). The existence of systematic errors in observed and proxy time series represents an important problem. Using only living trees from different stand types with particular historical harvesting (in our case—thinnings in the managed stands and the stand dynamics for natural forests) can turn into a source of errors. The use of samples extracted only from living trees has a potential limitation in climate reconstructions, because of age-dependent climate sensitivity (Esper et al. 2008). This could mean that annual growth rates of the same cambial age are not randomly distributed over time (Büntgen et al. 2010). These factors can have an overall limited bias in climate reconstructions (Esper et al. 2012).

The biological trend removal, using statistical methods, remains a challenging problem in dendrochronology, while the application of different detrending methods has the aim to preserve as much as possible the high- to low-frequency information. Most of the common individual detrending methods are limited to the preservation of climate induced low-frequency signal, at least above the mean segment length (Cook et al. 1995; Büntgen et al. 2010). Different statistical approaches were used for paleoclimatic reconstructions, but none of these are perfect (Sheppard 2010). Using samples with different lengths involves that calibration and verification statistics is only available for the well-replicated part of the chronologies, and this results in biased information about the long-term reconstruction robustness (Meko 1997; Martin-Benito et al. 2016).

4 Conclusions

Based on five local chronologies from the eastern limit of the natural distribution of beech forests in Europe, the June SPEI3 drought variability was reconstructed for the first time back to 1768. The regional beech chronology shows a significant and strong correlation with the June SPEI3 drought index, preserving inter-annual to inter-decadal variations. The spatial–temporal variability of the reconstructed June SPEI3, as captured by the stability maps, is stable and significant over Romania, the Republic of Moldova, and Ukraine, confirming in this way the local and the regional scale drought variability recorded by the beech tree-ring width. In the last 239 years, the wettest periods occurred

Table 6 Correlation with other hydroclimatic reconstructions

Hydroclimatic record	Location	Season	Correlation for the period and degrees of freedom (DoF)		
			1768–1899	1900–2007	1768–2007
Büntgen et al. (2010)	Slovakia	JJA	−0.16, DoF = 4	0.31, DoF = 5	0.00, DoF = 8
Solomina et al. (2005)	SW Crimea	AMJJ	−0.17, DoF = 2	0.43, DoF = 3	0.00, DoF = 4
Kern et al. (2013)	NE Hungary	pNov-cAug	−0.52, DoF = 3	0.38, DoF = 3	−0.29, DoF = 5
Griggs et al. (2007)	North Aegean	MJ	0.28, DoF = 4	−0.01, DoF = 5	0.20, DoF = 9
Levanič et al. (2013)	SW Romania	JJA	0.20, DoF = 3	0.67, DoF = 3	0.40, DoF = 5

in the following intervals: ~ 1795–1813, ~ 1903–1914, and ~ 1969–1982, while the driest periods occurred in the following intervals: ~ 1770–1790, ~ 1885–1900, ~ 1945–1968, and after ~ 1990. The occurrence of the extreme events in our reconstruction was confirmed by the different historical sources. We found a documentary mention of all 25 identified extreme events. Moreover, inter-annual variability of the tree-ring width variability in the Eastern part of Romania reflects the large-scale atmospheric circulation and Sea Surface Temperature during the April to June period. The high values of the TRW are associated with a high-pressure system over the northern Atlantic Ocean and north-western Europe, and with a low-pressure system over the south-western, central, and eastern Europe and with negative SST anomalies in the central and northern Atlantic Ocean. This circulation pattern favors the advection of the wet and cold air from the north-eastern and northern parts of the Atlantic Ocean to the central part of Europe, including our study site. In contrast, the low values of the TRW index are associated with a high-pressure system over Europe and a low-pressure system over the central part of the Atlantic Ocean, and with positive SST anomalies over the Mediterranean Sea and western coast of Africa and southern Europe. This different pattern, in turn, determines the advection of the dry and warm air which generates the drought conditions. Our results indicate that there is considerable potential to produce long and well-replicated beech chronologies in Romania which would allow new reconstructions of both regional drought and large-scale circulation variability over southern and central Europe, filling the knowledge gap and building a more complete image of the past climatic variability at continental scale.

Supplementary Information The online version contains supplementary material available at https://doi.org/10.1007/s00382-022-06255-8.

Acknowledgements C.-C.R., V.N., A.M. and I.P. were partially supported by EEA Financial Mechanism 2009–2014 under the project contract no 18SEE/2014; C.-C.R. and A.M. were, also partially supported by the EU cross-border project "Promote deadwood for resilient forests in the Romanian-Ukrainian cross border region" (RESFOR), no. 2SOFT/1.2/13. C.-C.R and V.N. were partially funded by Ministry of Research, Innovation and Digitalization within Program 1—Development of national research and development system, Subprogram 1.2—Institutional Performance—RDI excellence funding projects, under contract no. 10PFE/2021; M.I. and V.N. are supported by Helmholtz funding through the joint program "Changing Earth—Sustaining our Future" (PoF IV) program of the AWI. Funding by the AWI Strategy Fund Project—PalEX and by the Helmholtz Climate Initiative—REKLIM is gratefully acknowledged. V.N. was partially supported by a grant of the Ministry of Research, Innovation and Digitization, CNCS/CCCDI—UEFISCDI, project number PN-III-P1-1.1-PD-2019-0469, within PNCDI III. Also, we would like to thank Daniela Martole, for English proofreading.

Funding The open-access was funded only by Projekt DEAL, through Alfred Wegener Institute Helmholtz Centre for Polar and Marine Research.

References

AGERPRES (2020) Inundaţiile din 12–15 mai 1970. In: Agentia Natl. Presa AGERPRES

Akkemik Ü, Dağdeviren N, Aras A (2005) A preliminary reconstruction (A.D. 1635–2000) of spring precipitation using oak tree rings in the western Black Sea region of Turkey. Int J Biometeorol 49:297–302. https://doi.org/10.1007/s00484-004-0249-8

Bakke SJ, Ionita M, Tallaksen LM (2020) The 2018 northern European hydrological drought and its drivers in a historical perspective. Hydrol Earth Syst Sci 24:5621–5653. https://doi.org/10.5194/hess-24-5621-2020

Brázdil R, Stepánková P, Kyncl T, Kyncl J (2002) Fir tree-ring reconstruction of March–July precipitation in southern Moravia (Czech Republic), 1376–1996. Clim Res 20:223–239. https://doi.org/10.3354/cr020223

Briffa KR, Jones D (1990) Basic chronology statistics and assessment. Pages in E., editors. In: Cook ER, Kairiukstis L (eds) Methods of dendrochronology. Kluwer Academic Publishers, Dordrecht, pp 137–153

Bunn AG (2008) A dendrochronology program library in R (dplR). Dendrochronologia 26:115–124. https://doi.org/10.1016/j.dendro.2008.01.002

Büntgen U, Brázdil R, Frank D, Esper J (2010) Three centuries of Slovakian drought dynamics. Clim Dyn 35:315–329. https://doi.org/10.1007/s00382-009-0563-2

Büntgen U, Brázdil R, Dobrovolný P et al (2011) Five centuries of Southern Moravian drought variations revealed from living and historic tree rings. Theor Appl Climatol 105:167–180. https://doi.org/10.1007/s00704-010-0381-9

Buras A (2017) A comment on the expressed population signal. Dendrochronologia 44:130–132. https://doi.org/10.1016/j.dendro.2017.03.005

Busuioc A, Caian M, Cheval S et al (2010) Variabilitatea și schimbarea climei în România

Compo GP, Whitaker JS, Sardeshmukh PD (2006) Feasibility of a 100-year reanalysis using only surface pressure data. Bull Am Meteorol Soc 87:175–190. https://doi.org/10.1175/BAMS-87-2-175

Compo GP, Whitaker JS, Sardeshmukh PD et al (2011) The twentieth century reanalysis project. Q J R Meteorol Soc 137:1–28. https://doi.org/10.1002/qj.776

Cook ER, Kairiukstis LA (1990) Methods of dendrochronology: applications in the environmental sciences. Kluwer, Dordrecht

Cook ER, Peters K (1997) Calculating unbiased tree-ring indices for the study of climatic and environmental change. Holocene 7:361–370. https://doi.org/10.1177/095968369700700314

Cook ER, Briffa KR, Meko DM et al (1995) The 'segment length curse' in long tree-ring chronology development for palaeoclimatic studies. Holocene 5:229–237. https://doi.org/10.1177/095968369500500211

Cook ER, Seager R, Kushnir Y et al (2015) Old World megadroughts and pluvials during the common era. Sci Adv 1:e1500561. https://doi.org/10.1126/sciadv.1500561

Cook ER, Solomina O, Matskovsky V et al (2020) The European Russia drought atlas (1400–2016 CE). Clim Dyn 54:2317–2335. https://doi.org/10.1007/s00382-019-05115-2

Ciorba I (2015) Marea foamete din transilvania dintre anii 1813-1817 și impactul ei asupra mentalităților colective. Puterea memoriei. In: Şipoş S, Cepraga DO, Gumenâi I (eds) Tradiţii istorice româneşti şi perspective europene: in honorem academician Ioan-Aurel Pop. Editura Universității din Oradea: Oradea, Romania, pp 419–436. ISBN 978-606-10-1614-3

Cufar K, De Luis M, Eckstein D et al (2008) Reconstructing dry and wet summers in SE Slovenia from oak tree-ring series. Int J Biometeorol 52:607–615. https://doi.org/10.1007/s00484-008-0153-8

Dobrovolný P, Rybníček M, Kolář T et al (2018) May–July precipitation reconstruction from oak tree-rings for Bohemia (Czech Republic) since AD 1040. Int J Climatol 38:1910–1924. https://doi.org/10.1002/joc.5305

Dudaș F (1999) Catastrofe naturale în Transilvania. În: lumina ănsemnărilor scrise pe cărțile românești vechi între anii 1500 și 1900. Oradea, Romania

Ebisuzaki W (1997) A method to estimate the statistical significance of a correlation when the data are serially correlated. J Clim 10:2147–2153. https://doi.org/10.1175/1520-0442(1997)010%3c2147:AMTETS%3e2.0.CO;2

EDC (2013) Drought of 2003. In: Eur. Drought Cent. https://www.geo.uio.no/edc/droughtdb/edr/DroughtEvents/_2003_Event.php. Accessed 19 Nov 2020

Efron B, Tibshirani R (1986) Bootstrap methods for standard errors, confidence intervals, and other measures of statistical accuracy. Stat Sci 1:54–75. https://doi.org/10.1214/ss/1177013815

Esper J, Neuwirth B, Treydte K (2001) A new parameter to evaluate temporal signal strength of tree-ring chronologies. Dendrochronologia 19:10

Esper J, Frank D, Wilson R, Briffa KR (2005) Effect of scaling and regression on reconstructed temperature amplitude for the past millennium. Geophys Res Lett 32

Esper J, Niederer R, Bebi P, Frank D (2008) Climate signal age effects-Evidence from young and old trees in the Swiss Engadin. For Ecol Manage 255:3783–3789. https://doi.org/10.1016/j.foreco.2008.03.015

Esper J, Benz M, Pederson N (2012) Influence of wood harvest on tree-ring time-series of *Picea abies* in a temperate forest. For Ecol Manage 284:86–92. https://doi.org/10.1016/j.foreco.2012.07.047

Fritts HC (1976) Tree rings and climate. Academic Press, London

Garamszegi B, Kázmér M, Kolozs L, Kern Z (2020) Changing climatic sensitivity and effects of drought frequency on the radial growth of Fagus sylvatica at the xeric frontiers of central Europe. Idojaras 124:227–251. https://doi.org/10.28974/idojaras.2020.2.5

Griggs C, DeGaetano A, Kuniholm P, Newton M (2007) A regional high-frequency reconstruction of May–June precipitation in the north Aegean from oak tree rings, A.D. 1089–1989. Int J Climatol 27:1075–1089. https://doi.org/10.1002/joc.1459

Griggs C, Pearson C, Manning S, Lorentzen B (2014) A 250-year annual precipitation reconstruction and drought assessment for Cyprus from Pinus brutia Ten. tree-rings. Int J Climatol 34. https://doi.org/10.1002/joc.3869

Guiot J (1991) The bootstrapped method function. Tree Ring Bull 51:39–41

Haneca K, Čufar K, Beeckman H (2009) Oaks, tree-rings and wooden cultural heritage: a review of the main characteristics and applications of oak dendrochronology in Europe. J Archaeol Sci 36:1–11. https://doi.org/10.1016/j.jas.2008.07.005

Harris I, Osborn TJ, Jones P, Lister D (2020) Version 4 of the CRU TS monthly high-resolution gridded multivariate climate dataset. Sci Data 7:1–18. https://doi.org/10.1038/s41597-020-0453-3

Helama S, Sohar K, Läänelaid A et al (2018) Reconstruction of precipitation variability in Estonia since the eighteenth century, inferred from oak and spruce tree rings. Clim Dyn 50:4083–4101. https://doi.org/10.1007/s00382-017-3862-z

Ionita M (2015) Interannual summer streamflow variability over Romania and its connection to large-scale atmospheric circulation. Int J Climatol 35:4186–4196. https://doi.org/10.1002/joc.4278

Ionita M (2017) Mid range forecasting of the German Waterways streamflow based on hydrologic, atmospheric and oceanic data. Alfred-Wegener-Institut Helmholtz-Zentrum für Polar- und Meeresforschung, Bremerhaven, Germany

Ionita M, Nagavciuc V (2020) Forecasting low flow conditions months in advance through teleconnection patterns, with a special focus on summer 2018. Sci Rep 10:13258. https://doi.org/10.1038/s41598-020-70060-8

Ionita M, Nagavciuc V (2021) Changes in drought features at the European level over the last 120 years. Nat Hazards Earth Syst Sci 21:1685–1701. https://doi.org/10.5194/nhess-21-1685-2021

Ionita M, Lohmann G, Rimbu N (2008) Prediction of spring Elbe discharge Based on stable teleconnections with winter global temperature and precipitation. J Clim 21:6215–6226. https://doi.org/10.1175/2008JCLI2248.1

Ionita M, Lohmann G, Rimbu N et al (2012) Interannual to decadal summer drought variability over Europe and its relationship to global sea surface temperature. Clim Dyn 38:363–377. https://doi.org/10.1007/s00382-011-1028-y

Ionita M, Dima M, Lohmann G et al (2015) Predicting the June 2013 European flooding based on precipitation, soil moisture, and sea level pressure. J Hydrometeorol 16:598–614. https://doi.org/10.1175/JHM-D-14-0156.1

Ionita M, Grosfeld K, Scholz P et al (2019) September Arctic sea ice minimum prediction—a skillful new statistical approach. Earth Syst Dyn 10:189–203. https://doi.org/10.5194/esd-10-189-2019

Ionita M, Dima M, Nagavciuc V et al (2021) Past megadroughts in central Europe were longer, more severe and less warm than modern droughts. Commun Earth Environ 2:61. https://doi.org/10.1038/s43247-021-00130-w

IPCC (2018) Global Warming of 1.5°C. An IPCC special report on the impacts of global warming of 1.5°C above pre-industrial levels and related global greenhouse gas emission pathways, in the context of strengthening the global response to the threat of climate change. Geneva, Switzerland

Kern Z, Grynaeus A, Morgos A (2009) Reconstructed precipitation for southern Bakony Mountains (Transdanubia, Hungary) back to 1746 AD based on ring width of oak trees. Időjárás 113

Kern Z, Patkó M, Kázmér M et al (2013) Multiple tree-ring proxies (earlywood width, latewood width and δ13C) from pedunculate oak (*Quercus robur* L.), Hungary. Quat Int 293:257–267. https://doi.org/10.1016/j.quaint.2012.05.037

Köse N, Akkemik U, Güner H et al (2013) An improved reconstruction of May–June precipitation using tree-ring data from western Turkey and its links to volcanic eruptions. Int J Biometeorol 57:691–701. https://doi.org/10.1007/s00484-012-0595-x

Kozlowski TT, Pallardy G (1997) Growth control in woody plants. Elsevier, Amsterdam

Kress A, Saurer M, Siegwolf RTW et al (2010) A 350 year drought reconstruction from Alpine tree ring stable isotopes. Glob Biogeochem Cycles. https://doi.org/10.1029/2009GB003613

Levanič T, Popa I, Poljanšek S, Nechita C (2013) A 323-year long reconstruction of drought for SW Romania based on black pine (*Pinus Nigra*) tree-ring widths. Int J Biometeorol 57:703–714. https://doi.org/10.1007/s00484-012-0596-9

Martin-Benito D, Ummenhofer CC, Köse N et al (2016) Tree-ring reconstructed May–June precipitation in the Caucasus since 1752 CE. Clim Dyn 47:3011–3027. https://doi.org/10.1007/s00382-016-3010-1

Masson-Delmotte V, Raffalli-Delerce G, Danis PA et al (2005) Changes in European precipitation seasonality and in drought frequencies revealed by a four-century-long tree-ring isotopic record from Brittany, western France. Clim Dyn 24:57–69. https://doi.org/10.1007/s00382-004-0458-1

Meko D (1997) Dendroclimatic reconstruction with time varying predictor subsets of tree indices. J Clim 10:687–696. https://doi.org/10.1175/1520-0442(1997)010%3c0687:DRWTVP%3e2.0.CO;2

Meko D, Graybill DA (1995) Tree-ring reconstruction of upper Gila Rwer discharge. JAWRA J Am Water Resour Assoc 31:605–616. https://doi.org/10.1111/j.1752-1688.1995.tb03388.x

Mihailescu C (2004) Clima si harardele Moldovei. Evolutia, starea si predictia. Licorn, Chisinau

Nagavciuc V, Ionita M, Perșoiu A et al (2019a) Stable oxygen isotopes in Romanian oak tree rings record summer droughts and associated large-scale circulation patterns over Europe. Clim Dyn 52:6557–6568. https://doi.org/10.1007/s00382-018-4530-7

Nagavciuc V, Roibu C-C, Ionita M et al (2019b) Different climate response of three tree ring proxies of *Pinus sylvestris* from the Eastern Carpathians, Romania. Dendrochronologia 54:56–63

Nagavciuc V, Kern Z, Ionita M et al (2020) Climate signals in carbon and oxygen isotope ratios of Pinus cembra tree-ring cellulose from the Călimani Mountains, Romania. Int J Climatol 40:2539–2556. https://doi.org/10.1002/joc.6349

Pallardy S (2008) Physiology of woody plants, 3rd edn. Elsevier Academic Press, Amsterdam

Popa I, Cheval S (2007) Early winter temperature reconstruction of Sinaia area (Romania) derived from tree-rings of silver fir (*Abies alba* Mill.). Rom J Meteorol 9:47–54

Popa I, Kern Z (2009) Long-term summer temperature reconstruction inferred from tree ring records from the Eastern Carpathians. Clim Dyn 32:1107–1117

Popa I, Bouriaud O (2013) Reconstruction of summer temperatures in Eastern Carpathian Mountains (Rodna Mts, Romania) back to AD 1460 from tree-rings. Int J Climatol 34. https://doi.org/10.1002/joc.3730

Rayner NA, Parker DE, Horton EB et al (2003) Global analyses of sea surface temperature, sea ice, and night marine air temperature since the late nineteenth century. J Geophys Res Atmos. https://doi.org/10.1029/2002JD002670

Roibu CC, Popa I, Kirchhefer AJ, Palaghianu C (2017) Growth responses to climate in a tree-ring network of European beech (*Fagus sylvatica* L.) from the eastern limit of its natural distribution area. Dendrochronologia 42:104–116. https://doi.org/10.1016/j.dendro.2017.02.003

Roibu CC, Sfecla V, Mursa A et al (2020) The climatic response of tree ring width components of ash (*Fraxinus excelsior* L.) and common oak (*Quercus robur* L.) from Eastern Europe. Forests 11:600. https://doi.org/10.3390/F11050600

Roibu CC, Ważny T, Crivellaro A et al (2021) The Suceava oak chronology: a new 804 years long tree-ring chronology bridging the gap between central and south Europe. Dendrochronologia 68:125856. https://doi.org/10.1016/J.DENDRO.2021.125856

Sheppard PR (2010) Dendroclimatology: extracting climate from trees. Wiley Interdiscip Rev Clim Chang 1:343–352. https://doi.org/10.1002/wcc.42

Solomina O, Davi N, D'Arrigo R, Jacoby G (2005) Tree-ring reconstruction of Crimean drought and lake chronology correction. Geophys Res Lett 32:1–4. https://doi.org/10.1029/2005GL023335

Teodoreanu E (2017) În căutarea timpului trecut Schiță de climatologie istorică. Editura Paodeia: Bucuresti. ISBN 978-606-748-214-0

Topor N (1963) Anii ploioşi şi secetoşi din Republica Populară Romînă. C.S.A Institutul Meteorologic, Bucureşti

Touchan R, Akkemik Ü, Hughes MK, Erkan N (2007) May-June precipitation reconstruction of southwestern Anatolia, Turkey during the last 900 years from tree rings. Quat Res 68:196–202. https://doi.org/10.1016/j.yqres.2007.07.001

Van Lanen HAJ, Laaha G, Kingston DG et al (2016) Hydrology needed to manage droughts: the 2015 European case. Hydrol Process 30:3097–3104. https://doi.org/10.1002/hyp.10838

Vicente-Serrano SM, Beguería S, López-Moreno JI (2010) A multiscalar drought index sensitive to global warming: The standardized precipitation evapotranspiration index. J Clim 23:1696–1718. https://doi.org/10.1175/2009JCLI2909.1

Whitaker JS, Compo GP, Wei X, Hamill TM (2004) Reanalysis without radiosondes using ensemble data assimilation. Mon Weather Rev 132:1190–1200. https://doi.org/10.1175/1520-0493(2004)132%3c1190:RWRUED%3e2.0.CO;2

Wigley TML, Briffa KR, Jones PD (1984) On the average value of correlated time series, with applications in dendroclimatology and hydrometeorology. J Clim Appl Meteorol 23:201–213. https://doi.org/10.1175/1520-0450(1984)023%3c0201:OTAVOC%3e2.0.CO;2

von Wühlisch G (2008) Technical guidelines for genetic conservation and use *Fagus sylvatica* (European beech). Bioversity Int Rome (Italy)

Zang C, Biondi F (2015) treeclim: an R package for the numerical calibration of proxy-climate relationships. Ecography (cop) 38:431–436. https://doi.org/10.1111/ecog.01335

Zhao S, Pederson N, D'Orangeville L et al (2019) The international tree-ring data bank (ITRDB) revisited: data availability and global ecological representativity. J Biogeogr 46:355–368. https://doi.org/10.1111/jbi.13488